

# Effective field theory for type II seesaw model –symmetric phase v.s. broken phase–

---

Yi Liao<sup>a,b</sup> Xiao-Dong Ma<sup>a,b</sup> Yoshiki Uchida<sup>a,b</sup>

<sup>a</sup>State Key Laboratory of Nuclear Physics and Technology, Institute of Quantum Matter, South China Normal University, Guangzhou 510006, China

<sup>b</sup>Guangdong Basic Research Center of Excellence for Structure and Fundamental Interactions of Matter, Guangdong Provincial Key Laboratory of Nuclear Science, Guangzhou 510006, China

E-mail: [liaoy@m.scnu.edu.cn](mailto:liaoy@m.scnu.edu.cn), [maxid@scnu.edu.cn](mailto:maxid@scnu.edu.cn),  
[uchida.yoshiki@m.scnu.edu.cn](mailto:uchida.yoshiki@m.scnu.edu.cn)

ABSTRACT:

Effective field theory is an effective approach to parameterizing effects of high energy scale physics in low energy measurements. The two popular frameworks for physics beyond the standard model are the so-called standard model effective field theory (SMEFT) and the Higgs effective field theory (HEFT). While the description by the SMEFT deteriorates when the scale of new physics is not so high or it participates in spontaneous electroweak symmetry breaking, the HEFT makes use of nonlinear realization of spontaneously broken symmetry in which there are practically no restrictions on the Higgs field as a singlet. In this work we present another framework, called broken phase effective field theory (bEFT), in which we deal directly with mass eigenstate fields after spontaneous symmetry breaking without employing nonlinear realization. We take the type-II seesaw model as an example to demonstrate our approach. By matching the model to both the bEFT and the SMEFT at tree level, we compare the results for two processes, the Higgs pair production via vector boson fusion which appears as a subprocess at the LHC and the Higgs-strahlung process at a future electron-positron collider. We find that the bEFT reproduces the type-II seesaw model more accurately than the SMEFT in the regions where the bare mass of the Higgs triplet becomes close to the electroweak scale. Therefore, the bEFT serves as a useful framework that can compensate for the shortcomings in both the SMEFT and the HEFT when dealing with UV models that involve Higgs mixing or new particles with a mass close to the electroweak scale.

---

## Contents

<b>1</b>	<b>Introduction</b>	<b>2</b>
<b>2</b>	<b>Type-II seesaw model</b>	<b>4</b>
<b>3</b>	<b>Matching onto bEFT</b>	<b>6</b>
<b>4</b>	<b>Matching onto bSMEFT</b>	<b>7</b>
<b>5</b>	<b>List of Wilson coefficients for bEFT and bSMEFT operators</b>	<b>10</b>
<b>6</b>	<b>Numerical evaluation</b>	<b>12</b>
<b>7</b>	<b>Conclusion</b>	<b>19</b>
<b>A</b>	<b>Minimization of the scalar potential</b>	<b>20</b>

---

## 1 Introduction

With the discovery of the Higgs boson at the Large Hadron Collider (LHC) in 2012 [1, 2], the standard model (SM) was finally established. However, there are some problems that the SM cannot address, such as the origin of neutrino mass. In order to solve this problem, several types of new physics (NP) models have been proposed, such as the three conventional seesaw models [3–15] and radiative models aiming at a common origin of neutrino mass and dark matter [16, 17]; for a review see, e.g., Ref. [18]. Usually the new particles are much heavier than the electroweak scale, securing an effective field theory (EFT) approach to their effects in low energy physical processes.

There are two representative EFTs to parameterize the deviations caused by heavy NP from the SM predictions. One is the standard model effective field theory (SMEFT) [19–22]. In the SMEFT, the SM fields are classified by their representations in the complete gauge group  $G_{\text{SM}} = \text{SU}(3)_c \times \text{SU}(2)_L \times \text{U}(1)_Y$ . A perturbative expansion is performed in terms of  $1/\Lambda$ , where  $\Lambda$  denotes the NP scale. The leading-order interactions in the SMEFT consist of  $G_{\text{SM}}$  invariant operators up to mass dimension-four (dim-4), i.e. the SM Lagrangian. The other is the Higgs effective field theory (HEFT) [23–37]. In the HEFT the fields are classified by their representations in the unbroken gauge group  $\text{SU}(3)_c \times \text{U}(1)_{\text{em}}$ , but the  $\text{SU}(2)_L \times \text{U}(1)_Y$  symmetry is nonlinearly realized. Since the physical Higgs field  $h$  is now a singlet under this nonlinear symmetry, arbitrary functions of  $h$  appear in the HEFT Lagrangian. In this sense the HEFT already encodes deviations from the SM in the

leading order. In the HEFT, a perturbative expansion is done according to the number of loops.

Comparative studies have been actively carried out in recent years on matching a specific ultraviolet (UV) theory onto the SMEFT or the HEFT. For instance, Ref. [38] considers the SM extended with a real singlet scalar and matches it onto the SMEFT and the HEFT respectively. The matching of the two-Higgs-doublet model onto both the SMEFT and HEFT has also been performed [39–41]. In Refs. [42, 43], the SM extended with a real triplet scalar is matched onto the HEFT. See Refs. [35, 37, 44] for a more general discussion of theories that cannot be matched onto the SMEFT but must be matched onto the HEFT. The classification of the SMEFT and the HEFT in the context of a bottom-up approach is found in Refs. [45–49]. In general, if the NP scale is much higher than the electroweak scale, the new heavy fields are classified by their representations under  $G_{\text{SM}}$ . By integrating them out, the UV theory is matched to the SMEFT. On the other hand, if the NP scale is close to the electroweak scale, the mixing between the SM fields and the new heavy fields cannot be neglected. In this case, the theory should be written in terms of the degrees of freedom after the electroweak symmetry breaking (EWSB), and the original electroweak symmetry  $SU(2)_L \times U(1)_Y$  is nonlinearly realized. After bringing them to the mass eigenstates, the new heavy fields are integrated out, resulting in the HEFT.

In this paper, we introduce a new EFT framework that is different from both the SMEFT and the HEFT. In our framework, the UV theory is rewritten in terms of the degrees of freedom after the EWSB. We do not rewrite it in a nonlinearly realized form of  $SU(2)_L \times U(1)_Y$ , but instead work with the fields in the unitary gauge. After bringing the fields to their mass eigenstates, we integrate out the physical heavy fields. We call thus obtained EFT the broken phase EFT (bEFT). In the HEFT, the operators written in nonlinear realizations generate an infinite power of the fields, which complicates the evaluation of the physical observables. Our bEFT, on the other hand, does not include an infinite order terms of the fields and is therefore easier to deal with.

To illustrate our approach concretely, we consider matching the type-II seesaw model [9–14] onto our bEFT. In the type-II seesaw model, an  $SU(2)_L$  triplet scalar is introduced. Its vacuum expectation value (VEV) is severely constrained by the  $\rho$  parameter measurements. The lower bound on the mass of doubly charged scalars is around 400 GeV if the triplet VEV saturates the upper bound on the  $\rho$  parameter. If the NP scale is close to the electroweak scale, it is expected that the accuracy of the description by the SMEFT deteriorates. It is important to see whether the SMEFT or the bEFT can describe low-energy physics accurately in such a case. Matching the type-II seesaw onto the SMEFT has already been done up to dim-6 operators at the one-loop level in Ref. [50]. We rewrite its tree-level results in the basis after the EWSB, and call this EFT the broken phase SMEFT (bSMEFT). To assess which of the bEFT and bSMEFT can better reproduce the result of the UV theory, we consider two specific processes: one is the subprocess at the LHC

for the Higgs pair production through vector boson fusion  $W^-W^+ \rightarrow hh$ , and the other is the Higgsstrahlung process  $e^+e^- \rightarrow hZ$  at a future electron-positron collider. We show that the bEFT reproduces the cross sections of the UV theory more accurately than the bSMEFT over a wide range of parameter space. This is because the bEFT deals with the mass eigenstates after symmetry breaking and incorporates the mixing of scalar fields at the leading order.

This paper is organized as follows. We introduce the type-II seesaw model in Section 2. In Section 3, we describe how to perform its matching onto the bEFT. In Section 4, we rewrite the SMEFT matching results in a basis after the EWSB to get the bSMEFT. All operators up to dim-5 and some of dim-6 operators in the bEFT and bSMEFT are shown in Section 5. We then evaluate in Section 6 the two processes mentioned above in the UV theory, bEFT, and bSMEFT respectively and compare their results. We conclude in Section 7.

## 2 Type-II seesaw model

The type-II seesaw model adds a triplet scalar  $\Delta$  to the SM, with the Lagrangian given by

$$\mathcal{L}_{\text{UV}} = \mathcal{L}_{\text{SM}} + \text{Tr}[(D_\mu \Delta)^\dagger (D^\mu \Delta)] - \left[ \frac{1}{\sqrt{2}} Y_\Delta^{pr} \overline{L}_p^c i \sigma_2 \Delta L_r + \text{h.c.} \right] - \mathcal{V}(H, \Delta), \quad (2.1)$$

where the covariant derivative for  $\Delta$  is

$$D_\mu \Delta = \partial_\mu \Delta + i \frac{g}{2} [\sigma^a W_\mu^a, \Delta] + i g' B_\mu \Delta, \quad (2.2)$$

with  $W_\mu^a$  ( $a = 1, 2, 3$ ) and  $B_\mu$  denoting the  $\text{SU}(2)_L$  and  $\text{U}(1)_Y$  gauge fields, respectively. The scalar potential is given by

$$\begin{aligned} \mathcal{V}(H, \Delta) = & -m_H^2 (H^\dagger H) + \frac{\lambda}{2} (H^\dagger H)^2 + M_\Delta^2 \text{Tr}(\Delta^\dagger \Delta) + \frac{\lambda_1}{2} [\text{Tr}(\Delta^\dagger \Delta)]^2 \\ & + \frac{\lambda_2}{2} ([\text{Tr}(\Delta^\dagger \Delta)]^2 - \text{Tr}[(\Delta^\dagger \Delta)^2]) + \lambda_4 (H^\dagger H) \text{Tr}(\Delta^\dagger \Delta) \\ & + \lambda_5 H^\dagger [\Delta^\dagger, \Delta] H + \left( \frac{\Lambda_6}{\sqrt{2}} H^T i \sigma_2 \Delta^\dagger H + \text{h.c.} \right), \end{aligned} \quad (2.3)$$

where the notation follows Refs. [51, 52] and all parameters except for  $\Lambda_6$  are real. For simplicity, we will also assume  $\Lambda_6$  is real. The doublet scalar field develops a VEV  $v_H$ , which through the  $\Lambda_6$  coupling induces a VEV  $v_\Delta$  for the triplet scalar field:

$$H = \frac{1}{\sqrt{2}} \begin{pmatrix} \sqrt{2} w^+ \\ v_H + h_H + i z_0 \end{pmatrix}, \quad (2.4)$$

$$\Delta = \frac{\sigma^a}{\sqrt{2}} \Delta^a = \frac{1}{\sqrt{2}} \begin{pmatrix} \delta^+ & \sqrt{2} \delta^{++} \\ v_\Delta + \delta^0 + i \eta & -\delta^+ \end{pmatrix}, \quad (2.5)$$

where  $\Delta^1 = (\delta^{++} + \delta^0)/\sqrt{2}$ ,  $\Delta^2 = i(\delta^{++} - \delta^0)/\sqrt{2}$ , and  $\Delta^3 = \delta^+$ . The VEVs are obtained by the minimization conditions of the scalar potential to be detailed in Appendix A, and result in the scalar mixing:

$$\begin{pmatrix} G^\pm \\ H^\pm \end{pmatrix} = \begin{pmatrix} \cos \beta' & \sin \beta' \\ -\sin \beta' & \cos \beta' \end{pmatrix} \begin{pmatrix} w^\pm \\ \delta^\pm \end{pmatrix}, \quad (2.6a)$$

$$\begin{pmatrix} h \\ H_0 \end{pmatrix} = \begin{pmatrix} \cos \alpha & \sin \alpha \\ -\sin \alpha & \cos \alpha \end{pmatrix} \begin{pmatrix} h_H \\ \delta^0 \end{pmatrix}, \quad (2.6b)$$

$$\begin{pmatrix} G_0 \\ A_0 \end{pmatrix} = \begin{pmatrix} \cos \beta & \sin \beta \\ -\sin \beta & \cos \beta \end{pmatrix} \begin{pmatrix} z^0 \\ \eta \end{pmatrix}, \quad (2.6c)$$

where the mixing angles are given by

$$\tan \beta' = \frac{\sqrt{2}v_\Delta}{v_H}, \quad (2.7a)$$

$$\tan \beta = \frac{2v_\Delta}{v_H} = \sqrt{2} \tan \beta', \quad (2.7b)$$

$$\tan 2\alpha = \frac{4v_\Delta}{v_H} \frac{M_\Delta^2 + \frac{1}{2}\lambda_1 v_\Delta^2}{M_\Delta^2 + (\lambda_- - \lambda)v_H^2 + \frac{3}{2}\lambda_1 v_\Delta^2}, \quad (2.7c)$$

with

$$\lambda_- = \frac{1}{2}(\lambda_4 - \lambda_5). \quad (2.8)$$

The triplet VEV breaks the custodial symmetry, and is severely constrained by the precision  $\rho$  parameter. The latter is expressed in terms of the  $W$  boson mass  $M_W$ , the  $Z$  boson mass  $M_Z$ , and the Weinberg angle  $\theta_W$ :

$$\rho = \frac{M_W^2}{M_Z^2 \cos^2 \theta_W} = \frac{1}{1 + 2\epsilon^2}, \quad (2.9)$$

where

$$\epsilon = \frac{v_\Delta}{v_{ew}}, \quad (2.10)$$

and  $v_{ew} = \sqrt{v_H^2 + 2v_\Delta^2} \approx 246$  GeV. Allowing a  $3\sigma$  deviation from the measured value  $\rho_{\text{exp}} = 1.00038 \pm 0.00020$  [53], we obtain the upper bound  $\epsilon \leq 0.0105$ . In the following sections, we will work up to order  $\epsilon^2$ . We list here some interactions in the unitary gauge, including the ones relevant to later evaluation of the processes  $W^-W^+ \rightarrow hh$  and  $e^+e^- \rightarrow hZ$  in Section 6:

$$\begin{aligned} \mathcal{L}_{\text{UV}} \supset & C_{h^3}^{\text{UV}} h^3 + C_{hW^2}^{\text{UV}} h W_\mu^- W^{+\mu} + C_{h^2W^2}^{\text{UV}} h^2 W_\mu^- W^{+\mu} + C_{hZ^2}^{\text{UV}} h Z_\mu Z^\mu + C_{h^2Z^2}^{\text{UV}} h^2 Z_\mu Z^\mu \\ & + C_{h^2H_0}^{\text{UV}} h^2 H_0 + C_{H_0W^2}^{\text{UV}} H_0 W_\mu^- W^{+\mu} + C_{H_0Z^2}^{\text{UV}} H_0 Z_\mu Z^\mu \\ & + (C_{hHW}^{\text{UV}} (H^+ \overleftrightarrow{D}_\mu h) W^{-\mu} + \text{h.c.}) + C_{hA_0Z}^{\text{UV}} (A_0 \overleftrightarrow{\partial}_\mu h) Z^\mu, \end{aligned} \quad (2.11)$$

where  $\Phi_1 \overleftrightarrow{D}_\mu \Phi_2 \equiv \Phi_1 D_\mu \Phi_2 - (D_\mu \Phi_1) \Phi_2$ , and the coefficients are

$$C_{h^3}^{\text{UV}} = -\frac{\lambda}{2} v_{\text{ew}} + \epsilon^2 v_{\text{ew}} \left[ \frac{(6\kappa^3 - 2\kappa^2 + \kappa - 1)}{2r_\Delta^2 \kappa} - \frac{\lambda_-(2\kappa^2 - 1)}{2} \right], \quad (2.12\text{a})$$

$$C_{hW^2}^{\text{UV}} = \frac{g^2 v_{\text{ew}}}{2} [1 + \epsilon^2 (-2\kappa^2 + 4\kappa - 1)], \quad (2.12\text{b})$$

$$C_{h^2 W^2}^{\text{UV}} = \frac{g^2}{4} [1 + 4\epsilon^2 \kappa^2], \quad (2.12\text{c})$$

$$C_{hZ^2}^{\text{UV}} = \frac{g^2 v_{\text{ew}}}{4c_W^2} [1 + \epsilon^2 (-2\kappa^2 + 8\kappa - 1)], \quad (2.12\text{d})$$

$$C_{h^2 Z^2}^{\text{UV}} = \frac{g^2}{8c_W^2} [1 + 12\epsilon^2 \kappa^2], \quad (2.12\text{e})$$

$$C_{h^2 H_0}^{\text{UV}} = \epsilon v_{\text{ew}} \frac{3\kappa - 2 - \lambda_- \kappa r_\Delta^2}{r_\Delta^2}, \quad (2.12\text{f})$$

$$C_{H_0 W^2}^{\text{UV}} = -g^2 \epsilon (\kappa - 1) v_{\text{ew}}, \quad (2.12\text{g})$$

$$C_{H_0 Z^2}^{\text{UV}} = -\epsilon v_{\text{ew}} \frac{g^2 (\kappa - 2)}{2c_W^2}, \quad (2.12\text{h})$$

$$C_{hHW}^{\text{UV}} = \epsilon \frac{g(2\kappa - 1)}{\sqrt{2}}, \quad (2.12\text{i})$$

$$C_{hA_0 Z}^{\text{UV}} = \epsilon \frac{g(2\kappa - 1)}{c_W}, \quad (2.12\text{j})$$

where

$$r_\Delta = \frac{v_{\text{ew}}}{M_\Delta}, \quad \kappa = \frac{1}{1 + r_\Delta^2 (\lambda_- - \lambda)}. \quad (2.13)$$

One notices that the new contributions from the triplet scalar are suppressed by  $\mathcal{O}(\epsilon)$  or  $\mathcal{O}(\epsilon^2)$  relative to the SM parts.

### 3 Matching onto bEFT

In this section, we perform the matching of the type-II seesaw model onto the bEFT at tree level. As we emphasized in Section 1, the bEFT introduced in this work differs from the HEFT in several ways. The HEFT employs a perturbative expansion in the number of loops. Our bEFT, on the other hand, employs double expansions in terms of both  $\epsilon$  and the inverse of heavy fields' masses. In addition, the HEFT introduces the would-be Goldstone fields in a nonlinear realization, while our bEFT assumes the unitary gauge and removes the would-be Goldstone fields from the very start. We take the new scalars  $H_0$ ,  $A_0$ ,  $H^\pm$ , and  $H^{\pm\pm}$  as heavy states and integrate them out to perform matching onto the bEFT.

Before going into the details, we introduce an auxiliary  $\mathbb{Z}_2$  parity that can help book-keep the power of expansion on the matching. Under the  $\mathbb{Z}_2$  the triplet scalar and the

couplings  $Y_\Delta$ ,  $\Lambda_6$  flip sign,  $(\Delta, Y_\Delta, \Lambda_6) \rightarrow -(\Delta, Y_\Delta, \Lambda_6)$ , while the SM fields and other couplings keep intact. This symmetry is preserved in the broken phase since the triplet VEV being proportional to  $\Lambda_6$  is also odd under the  $\mathbb{Z}_2$ , i.e.,  $v_\Delta \rightarrow -v_\Delta$  or  $\epsilon \rightarrow -\epsilon$ . The solutions of the equations of motion for the heavy scalar fields  $\Phi \in \{H_0, A_0, H^\pm, H^{\pm\pm}\}$  are expressed in terms of the SM fields in the mass eigenstates. The odd parity of the heavy fields implies the solutions in the form:

$$\Phi_c[\phi_{\text{SM}}] = \sum_{m=0}^{\infty} \sum_{n=0}^{2m+1} \epsilon^n Y_\Delta^{2m+1-n} \mathcal{O}^{(m,n)}[\phi_{\text{SM}}], \quad (3.1)$$

where  $\mathcal{O}^{(m,n)}[\phi_{\text{SM}}]$  is an operator composed only of the SM fields  $\phi_{\text{SM}}$ . Our goal is to match the type-II seesaw model onto the bEFT up to dim-6 and order  $\epsilon^2$ . In light of the fact that  $\mathcal{O}^{(m,n)}[\phi_{\text{SM}}]$  contains lepton bilinears  $(\bar{l}_1 l_2)^{2m+1-n}$  with  $l = \ell, \nu$ , we can easily check that the following three terms in the scalar potential,

$$\mathcal{V}^{\text{bEFT}}[h, \Phi_c] \supset \tilde{\lambda}_1 \epsilon \Phi_c^3 + \tilde{\lambda}_2 \epsilon h \Phi_c^3 + \tilde{\lambda}_3 \Phi_c^4, \quad (3.2)$$

only generate operators of dim- $n$  ( $n \geq 7$ ) and/or of order  $\epsilon^n$  ( $n \geq 3$ ), and are therefore irrelevant. Here  $\tilde{\lambda}_i$  ( $i = 1, 2, 3$ ) is given by a function of parameters in the original Lagrangian. The remaining interactions relevant to our analysis are given by

$$\begin{aligned} \mathcal{V}^{\text{UV}}[h, \Phi] \supset & \frac{m_h^2}{2} h^2 + \frac{m_{H_0}^2}{2} H_0^2 + \frac{m_{A_0}^2}{2} A_0^2 + m_{H^\pm}^2 H^- H^+ + m_{H^{\pm\pm}}^2 H^{--} H^{++} \\ & + \frac{1}{2} (2v_{\text{ew}} h + h^2) [\lambda_- H_0^2 + \lambda_- A_0^2 + (2\lambda_- + \lambda_5) H^- H^+ + 2(\lambda_- + \lambda_5) H^{--} H^{++}] \\ & + \epsilon v_{\text{ew}} \left[ \frac{M_\Delta^2 (2 - 3\kappa)}{v_{\text{ew}}^2} + \lambda_- \kappa \right] h^2 H_0 + \epsilon \left[ \frac{M_\Delta^2 (1 - \kappa)}{v_{\text{ew}}^2} + \lambda_- \kappa \right] h^3 H_0, \end{aligned} \quad (3.3)$$

and the kinetic energy terms of heavy fields. We can now integrate out heavy scalar fields  $H_0, A_0, H^\pm$ , and  $H^{\pm\pm}$  to obtain the bEFT up to the dim-6 level. This may be accomplished with the help of the Mathematica package `Matchete` [54]. The resulting effective operators and their Wilson coefficients (WCs) are listed in Section 5.

## 4 Matching onto bSMEFT

In this section, we consider matching the type-II seesaw model onto the SMEFT and rewrite it in terms of the fields in the broken phase to get the bSMEFT. We emphasize here that the bEFT in the previous section is obtained by integrating out heavy fields after the EWSB, whereas the bSMEFT is obtained by integrating out heavy fields before the EWSB. The tree level matching result onto the SMEFT can be found in Ref. [50], which is given by

$$\begin{aligned} \mathcal{L}_{\text{SMEFT}}^{\text{dim6}} = & \mathcal{L}_{\text{SM}} + \frac{\Lambda_6^2}{2M_\Delta^2} \left( 1 - \frac{2m_H^2}{M_\Delta^2} \right) (H^\dagger H)^2 + (C_{pr}^{(5)} \mathcal{O}_{pr}^{(5)} + \text{h.c.}) \\ & + C_{\ell\ell}^{prst} \mathcal{O}_{\ell\ell}^{prst} + C_H \mathcal{O}_H + C_{H\Box} \mathcal{O}_{H\Box} + C_{HD} \mathcal{O}_{HD} \end{aligned}$$

$$+ (C_{eH}^{pr} \mathcal{O}_{eH}^{pr} + C_{uH}^{pr} \mathcal{O}_{uH}^{pr} + C_{dH}^{pr} \mathcal{O}_{dH}^{pr} + \text{h.c.}), \quad (4.1)$$

where the dim-5 Weinberg operator is  $\mathcal{O}_{pr}^{(5)} = \bar{L}^p \tilde{H} \tilde{H}^T L^r c$  and the remaining dim-6 operators adopt the standard Warsaw basis notation [22]. The matched WCs are given by

$$\begin{aligned} C_{pr}^{(5)} &= -\frac{\Lambda_6 Y_{\Delta}^{*pr}}{2M_{\Delta}^2}, & C_{\ell\ell}^{prst} &= \frac{Y_{\Delta}^{*ps} Y_{\Delta}^{rt}}{4M_{\Delta}^2}, \\ C_H &= (4\lambda - \lambda_-) \frac{\Lambda_6^2}{M_{\Delta}^4} - \frac{\Lambda_6^4}{M_{\Delta}^6}, \\ C_{H\Box} &= \frac{\Lambda_6^2}{2M_{\Delta}^4}, & C_{HD} &= \frac{\Lambda_6^2}{M_{\Delta}^4}, \\ C_{eH}^{pr} &= \frac{\Lambda_6^2 Y_l^{pr}}{2M_{\Delta}^4}, & C_{uH}^{pr} &= \frac{\Lambda_6^2 Y_u^{pr}}{2M_{\Delta}^4}, & C_{dH}^{pr} &= \frac{\Lambda_6^2 Y_d^{pr}}{2M_{\Delta}^4}, \end{aligned} \quad (4.2a)$$

where the superscripts  $p, r, s, t$  denote fermion generations. Note that  $\Lambda_6$  is considered as the same order as the bare mass  $M_{\Delta}$  in the SMEFT power counting.  $Y_l^{pr}$ ,  $Y_u^{pr}$ , and  $Y_d^{pr}$  are the SM Yukawa couplings for the charged leptons, up-type quarks, and down-type quarks, respectively. In the following part, we will rewrite the above SMEFT interactions in terms of the broken phase fields to get the bSMEFT.

### Shift of VEV

The scalar potential is modified by the inclusion of the dim-6 operator  $\mathcal{O}_H$ :

$$\mathcal{V}_{\text{SMEFT}}^{\text{dim6}} = -m_H^2 H^\dagger H + \frac{\lambda_{\text{eff}}}{2} (H^\dagger H)^2 - C_H (H^\dagger H)^3, \quad (4.3)$$

with

$$\lambda_{\text{eff}} = \lambda - \frac{\Lambda_6^2}{M_{\Delta}^2} \left( 1 - \frac{2m_H^2}{M_{\Delta}^2} \right). \quad (4.4)$$

The dimensionful parameter  $\Lambda_6$  can be expressed in terms of  $v_H$  and  $v_{\Delta}$  by Eq. (A.4b):

$$\Lambda_6 = \frac{2M_{\Delta}^2 v_{\Delta} + \lambda_1 v_{\Delta}^3 + 2\lambda_- v_{\Delta} v_H^2}{v_H^2}. \quad (4.5)$$

The solution for the new minimum is given by

$$\langle H^\dagger H \rangle = \frac{\lambda_{\text{eff}} - \sqrt{\lambda_{\text{eff}}^2 - 6C_H \lambda_{\text{eff}} v_H^2}}{6C_H}. \quad (4.6)$$

We expand the above solution to the first order of  $C_H$  and define the new vacuum as

$$\langle H^\dagger H \rangle = \frac{v_H^2}{2} \left( 1 + \frac{3C_H v_H^2}{2\lambda_{\text{eff}}} \right) \equiv \frac{\tilde{v}_{\text{ew}}^2}{2}. \quad (4.7)$$

Note that  $\tilde{v}_{\text{ew}}$  can be expressed in terms of the potential parameters as

$$\tilde{v}_{\text{ew}}^2 = v_H^2 \left[ 1 + \frac{6(14\lambda - \lambda_-)(M_\Delta^2 + \lambda_- v_H^2)^2}{\lambda M_\Delta^4} \frac{v_\Delta^2}{v_H^2} + \mathcal{O}(v_\Delta^3/v_H^3) \right]. \quad (4.8)$$

We emphasize that, as the notation suggests, the above expression for  $\tilde{v}_{\text{ew}}$  is different from that for  $v_{\text{ew}}$  introduced in Eq. (A.2) for the UV theory, although they are numerically identical:  $v_{\text{ew}} = \tilde{v}_{\text{ew}} = 246 \text{ GeV}$ . In the following, as we did for the UV theory in Section 2, we expand the bSMEFT in terms of the parameter

$$\tilde{\epsilon} = \frac{v_\Delta}{\tilde{v}_{\text{ew}}}. \quad (4.9)$$

### Higgs-gauge interactions

The interactions between the Higgs and gauge bosons are modified by the dim-6 operators  $\mathcal{O}_{H\Box}$  and  $\mathcal{O}_{HD}$  which will change the normalization of the Higgs field. Redefining the Higgs field to make it canonically normalized will modify all interactions involving the Higgs field. The relevant terms are

$$\mathcal{L}_{\text{SMEFT}}^{H,\text{kin}} = (D_\mu H)^\dagger D^\mu H + C_{H\Box} \mathcal{O}_{H\Box} + C_{HD} \mathcal{O}_{HD}, \quad (4.10)$$

yielding the derivative terms of the Higgs field  $h_H$ :

$$\mathcal{L}_{\text{SMEFT}}^{H,\text{kin}} \supset \frac{1}{2} \left[ 1 - 2c_{\text{kin}} \left( 1 + \frac{h_H}{\tilde{v}_{\text{ew}}} \right)^2 \right] \partial_\mu h_H \partial^\mu h_H, \quad (4.11)$$

where

$$c_{\text{kin}} = \tilde{v}_{\text{ew}}^2 C_{H\Box} - \frac{1}{4} \tilde{v}_{\text{ew}}^2 C_{HD} = \tilde{\epsilon}^2 (1 + \lambda_- \tilde{r}_\Delta^2)^2, \quad \tilde{r}_\Delta \equiv \frac{\tilde{v}_{\text{ew}}}{M_\Delta}. \quad (4.12)$$

The Higgs field is made canonically normalized by rescaling

$$\tilde{h} = h_H \sqrt{1 - 2c_{\text{kin}}} \approx h_H (1 - c_{\text{kin}}). \quad (4.13)$$

By substituting Eq. (4.13) into Eq. (4.10), we get modified Higgs-gauge interactions.

### Higgs self-interactions

The Higgs self-interactions are modified by the operator  $\mathcal{O}_H$ , as well as by the Higgs field redefinition through the  $\mathcal{O}_{H\Box}$  and  $\mathcal{O}_{HD}$  operators. The final form of the scalar potential in the broken phase is given by

$$\begin{aligned} \mathcal{L}_{\text{SMEFT}}^{\text{dim6}} \supset & -\frac{\lambda_{\text{eff}}}{2} \tilde{v}_{\text{ew}}^2 \left( 1 - \frac{3C_H v_H^2}{\lambda_{\text{eff}}} + 2c_{\text{kin}} \right) \tilde{h}^2 - \frac{\lambda_{\text{eff}}}{2} \tilde{v}_{\text{ew}} \left( 1 - \frac{5C_H \tilde{v}_{\text{ew}}^2}{\lambda_{\text{eff}}} + 3c_{\text{kin}} \right) \tilde{h}^3 \\ & - \frac{\lambda_{\text{eff}}}{8} \left( 1 - \frac{15C_H \tilde{v}_{\text{ew}}^2}{\lambda_{\text{eff}}} + 4c_{\text{kin}} \right) \tilde{h}^4 + \frac{3}{4} C_H v_H \tilde{h}^5 + \frac{1}{8} C_H \tilde{h}^6. \end{aligned} \quad (4.14)$$

dim-3		
Operator	WC in bEFT	WC in bSMEFT
$\Delta L = 0$		
$h^3$	$-\frac{\lambda}{2}v_{\text{ew}} + \epsilon^2 v_{\text{ew}} \left[ \frac{(1-2\kappa^2)\lambda_-}{2} - \frac{1-\kappa+2\kappa^2-6\kappa^3}{2\kappa r_\Delta^2} \right]$	$-\frac{\lambda}{2}\tilde{v}_{\text{ew}} + \tilde{\epsilon}^2 \tilde{v}_{\text{ew}} \left[ \frac{2}{\tilde{r}_\Delta^2} + \frac{73}{2}\lambda - 6\lambda_- + \lambda_-(73\lambda - 18\lambda_-)\tilde{r}_\Delta^2 \right]$
$hW_\mu^- W^{+\mu}$	$\frac{g^2 v_{\text{ew}}}{2} [1 - \epsilon^2(1 - 4\kappa + 2\kappa^2)]$	$\frac{g^2 \tilde{v}_{\text{ew}}}{2} [1 + \tilde{\epsilon}^2(1 + 2\lambda_- \tilde{r}_\Delta^2)]$
$hZ_\mu Z^\mu$	$\frac{g^2 v_{\text{ew}}}{4c_W^2} [1 - \epsilon^2(1 - 8\kappa + 2\kappa^2)]$	$\frac{g^2 \tilde{v}_{\text{ew}}}{4c_W^2} [1 + 5\tilde{\epsilon}^2(1 + 2\lambda_- \tilde{r}_\Delta^2)]$
$\Delta L = 2$		
$\overline{\nu_{L,p}^c} \nu_{L,r}$	$-\epsilon \frac{v_{\text{ew}}}{2} Y_\Delta^{pr}$	$-\tilde{\epsilon} \frac{\tilde{v}_{\text{ew}}}{2} Y_\Delta^{pr} [1 + \lambda_- \tilde{r}_\Delta^2]$

**Table 1.** WCs for the dim-3 operators in the bEFT and bSMEFT.

### Yukawa interactions and neutrino mass

The Yukawa interactions are modified by the operator  $\mathcal{O}_{\psi H}^{pr}$  ( $\psi = u, d, e$ ). Including the Higgs field redefinition, they become

$$\mathcal{L}_{\text{SMEFT}}^{\text{dim6}} \supset -\frac{\tilde{v}_{\text{ew}}}{\sqrt{2}} \left( 1 + (1 + c_{\text{kin}}) \frac{\tilde{h}}{\tilde{v}_{\text{ew}}} \right) \sum_{\psi=u,d,e} \left[ Y_\psi^{pr} - \frac{C_{\psi H}^{pr} \tilde{v}_{\text{ew}}^2}{2M_\Delta^2} \left( 1 + \frac{\tilde{h}}{\tilde{v}_{\text{ew}}} \right)^2 \right] \bar{\psi}_L^p \psi_R^r + \text{h.c.} . \quad (4.15)$$

The neutrino mass and neutrino Yukawa interactions are induced by the dim-5 operator  $\mathcal{O}_{pr}^{(5)}$ , which become in the broken phase

$$C_{pr}^{(5)} \mathcal{O}_{pr}^{(5)} + \text{h.c.} = -\frac{\tilde{v}_{\text{ew}}^2}{2} C_{pr}^{(5)} \left( 1 + \frac{\tilde{h}}{\tilde{v}_{\text{ew}}} \right)^2 \overline{\nu_{L,p}^c} \nu_{L,r} + \text{h.c.} . \quad (4.16)$$

## 5 List of Wilson coefficients for bEFT and bSMEFT operators

In this section we list the WCs of the effective operators in the bEFT and bSMEFT. In all tables the second column lists the WCs for the operators in the bEFT up to order  $\epsilon^2$ , while the third column lists those in the bSMEFT up to order  $\tilde{\epsilon}^2$  and  $\tilde{r}_\Delta^2$ . The field  $h$  in the third column corresponds to the canonically normalized  $\tilde{h}$  in Sec. 4. Note that the Hermitian conjugate of a non-Hermitian operator is not listed.

In Table 1 and Table 2, we list the coefficients of the lepton-number-conserving ( $\Delta L = 0$ ) and -violating ( $\Delta L = 2$ ) dim-3 and dim-4 operators, respectively. Notice that we have expressed the matched WCs in both EFTs in terms of the common set of parameters in order to facilitate numerical comparison. The heavy masses in WCs of the bEFT have been replaced by the chosen parameters that make them look a little bit complicated. As can be seen from Table 1, all the coefficients of dim-3 operators in the bEFT coincide with those in the UV. From these tables, the deviations from the SM in the Higgs-gauge and pure-gauge

dim-4		
Operator	WC in bEFT	WC in bSMEFT
$\Delta L = 0$		
$h^4$	$-\frac{\lambda}{8} - \epsilon^2 \left[ \frac{(1-\kappa)\kappa}{r_\Delta^2} + \kappa^2 \lambda_- + \frac{(2-3\kappa + \kappa \lambda_- r_\Delta^2)^2}{2(1+\lambda_- r_\Delta^2)r_\Delta^2} \right]$	$-\frac{\lambda}{8} + \epsilon^2 \left[ \frac{1}{2\tilde{r}_\Delta^2} + 29\lambda - \frac{13}{2}\lambda_- + \frac{29}{2}\lambda_-(4\lambda - \lambda_-)\tilde{r}_\Delta^2 \right]$
$h^2 W_\mu^- W^{+\mu}$	$\frac{g^2}{4} \left[ 1 - \epsilon^2 \frac{4(1-2\kappa)(2-\kappa + \kappa \lambda_- r_\Delta^2)}{1 + \lambda_- r_\Delta^2} \right]$	$\frac{g^2}{4} [1 + 2\epsilon^2(1 + 2\tilde{r}_\Delta^2 \lambda_-)]$
$h^2 Z_\mu Z^\mu$	$\frac{g^2}{8c_W^2} \left[ 1 - \epsilon^2 \frac{8(1-2\kappa)(2 + \kappa \lambda_- r_\Delta^2)}{1 + \lambda_- r_\Delta^2} \right]$	$\frac{g^2}{8c_W^2} [1 + 14\epsilon^2(1 + 2\tilde{r}_\Delta^2 \lambda_-)]$
$W_\mu^- W^{+\mu} W_\nu^- W^{+\nu}$	$-\frac{g^4}{2} \left[ 1 - \epsilon^2 \frac{(1-\kappa)^2 r_\Delta^2}{1 + \lambda_- r_\Delta^2} \right]$	$-\frac{g^4}{2}$
$W_\mu^- W_\nu^+ W^{-\mu} W^{+\nu}$	$\frac{g^4}{2} \left[ 1 + \epsilon^2 \frac{r_\Delta^2}{1 + \lambda_- r_\Delta^2} \right]$	$\frac{g^4}{2}$
$W_\mu^- W^{+\mu} Z_\nu Z^\nu$	$-g^4 c_W^2 \left[ 1 - \epsilon^2 \frac{(2-\kappa)(1-\kappa)r_\Delta^2}{2c_W^4(1 + \lambda_- r_\Delta^2)} \right]$	$-g^4 c_W^2$
$W_\mu^- W_\nu^+ Z^\mu Z^\nu$	$g^4 c_W^2 \left[ 1 + \epsilon^2 \frac{r_\Delta^2}{c_W^4(2 + (2\lambda_- + \lambda_5)r_\Delta^2)} \right]$	$g^4 c_W^2$
$Z_\mu Z^\mu Z_\nu Z^\nu$	$\epsilon^2 \frac{g^4(2-\kappa)^2 r_\Delta^2}{8c_W^4(1 + \lambda_- r_\Delta^2)}$	0
$h\bar{\psi}_{L,p}\psi_{R,r}(\psi = u, d, e)$	$-\frac{1}{\sqrt{2}}Y_\psi^{pr}$	$-\frac{1}{\sqrt{2}}Y_\psi^{pr} [1 - 2\epsilon^2(1 + 2\lambda_- \tilde{r}_\Delta^2)]$
$\Delta L = 2$		
$h(\overline{\nu_{L,p}^c} \nu_{L,r})$	$-\tilde{\epsilon}Y_\Delta^{pr}(1 + \lambda_- r_\Delta^2)$	$-\tilde{\epsilon}Y_\Delta^{pr}(1 + \lambda_- \tilde{r}_\Delta^2)$

**Table 2.** WCs for the dim-4 operators in the bEFT and bSMEFT.

interactions are of order  $\epsilon^2$  ( $\tilde{\epsilon}^2$ ) in the bEFT (bSMEFT). This can be understood from the  $\mathbb{Z}_2$  symmetry introduced in Section 3. The expressions for the neutrino mass differ between the bSMEFT and the bEFT. This is because in the bSMEFT the neutrino mass term arises through the Weinberg operator, whereas in the bEFT the neutrino mass appears already before integrating out heavy fields through the mixing among scalar fields. Note that the  $W^4$ ,  $W^2 Z^2$ , and  $Z^4$  interactions in the bSMEFT coincide with those in the SM as can be seen in Table 2. This is because the pure gauge operators without derivatives are generated only through the product of the  $D_\mu H$ , so that the corrections to these interactions start to arise only from the dim-8 operators.

In Table 3 we list the WCs of both lepton-number-conserving and lepton-number-violating dim-5 operators in the bEFT and bSMEFT. Similar comments to the above quartic  $W$ ,  $Z$  operators apply to the dim-5 pure bosonic operators as well. Note that the bSMEFT includes  $h^3 Z^2$  but not  $h^3 W^2$  interactions, reflecting custodial symmetry breaking by  $\mathcal{O}_{HD}$ . And finally in Table 4, we show the WCs of the dim-6 operators in the bEFT and the bSMEFT that are relevant to the  $W^- W^+ \rightarrow hh$ ,  $ZZ \rightarrow hh$ , and  $e^+ e^- \rightarrow hZ$  scattering processes, two of which will be computed in the next section.

dim-5		
Operator	WC in bEFT	WC in bSMEFT
$\Delta L = 0$		
$h^5$	$\frac{\epsilon^2[(1-\kappa)(2-3\kappa)r_\Delta^{-2} - 2(1-5\kappa+5\kappa^2)\lambda_- - (1-3\kappa)\kappa\lambda_-^2 r_\Delta^2]}{v_{\text{ew}}(1+\lambda_- r_\Delta^2)^2}$	$\frac{3\tilde{\epsilon}^2}{\tilde{v}_{\text{ew}}}(4\lambda_- - \lambda_-)(1+2\lambda_- \tilde{r}_\Delta^2)$
$h^3 W_\mu^- W^{+\mu}$	$\frac{\epsilon^2 g^2[-1+2\kappa^2+(1-\kappa)(3-8\kappa)\lambda_- r_\Delta^2 + (1-2\kappa)\kappa\lambda_-^2 r_\Delta^4]}{v_{\text{ew}}(1+\lambda_- r_\Delta^2)^2}$	0
$h W_\mu^- W^{+\mu} W_\nu^- W^{+\nu}$	$\frac{\epsilon^2 g^4(1-\kappa)[\kappa r_\Delta^2 - (1-2\kappa)\lambda_- r_\Delta^4]}{v_{\text{ew}}(1+\lambda_- r_\Delta^2)^2}$	0
$h W_\mu^- W_\nu^+ W^- W^{+\nu}$	$\frac{\epsilon^2 g^4[2\kappa r_\Delta^2 - (1-2\kappa)\lambda_- r_\Delta^4]}{v_{\text{ew}}(1+(\lambda_- + \lambda_5)r_\Delta^2)^2}$	0
$h^3 Z_\mu Z^\mu$	$\frac{\epsilon^2 g^2[-2-3\kappa+8\kappa^2+3(2-7\kappa+4\kappa^2)\lambda_- r_\Delta^2 + 2(1-2\kappa)\kappa\lambda_-^2 r_\Delta^4]}{2v_{\text{ew}}c_W^2(1+\lambda_- r_\Delta^2)^2}$	$\frac{\tilde{\epsilon}^2 g^2(1+2\lambda_- \tilde{r}_\Delta^2)}{\tilde{v}_{\text{ew}}c_W^2}$
$h Z_\mu Z^\mu Z_\nu Z^\nu$	$\frac{\epsilon^2 g^4(2-\kappa)[3\kappa r_\Delta^2 - 2(1-2\kappa)\lambda_- r_\Delta^4]}{4v_{\text{ew}}c_W^4(1+\lambda_- r_\Delta^2)^2}$	0
$h W_\mu^- W^{+\mu} Z_\nu Z^\nu$	$\frac{\epsilon^2 g^4[(5-4\kappa)\kappa r_\Delta^2 - (4-11\kappa+6\kappa^2)\lambda_- r_\Delta^4]}{2v_{\text{ew}}c_W^2(1+\lambda_- r_\Delta^2)^2}$	0
$h W_\mu^- W_\nu^+ Z^\mu Z^\nu$	$\frac{2\epsilon^2 g^4[2(1-c_W^2-4\kappa+2\kappa c_W^2)r_\Delta^2 + (2-c_W^2)(1-2\kappa)\lambda_4 r_\Delta^4]}{v_{\text{ew}}c_W^2(2+(2\lambda_- + \lambda_5)r_\Delta^2)^2}$	0
$ih W_\mu^- W_\nu^+ Z^{\mu\nu}$	$-\frac{\epsilon^2 g^3(1-2\kappa)r_\Delta^2}{v_{\text{ew}}c_W(2+(2\lambda_- + \lambda_5)r_\Delta^2)}$	0
$(hi\overleftrightarrow{D}_\mu W_\nu^-)W^{+\mu}Z^\nu$	$\frac{\epsilon^2 g^3(1-2\kappa)r_\Delta^2}{v_{\text{ew}}c_W(2+(2\lambda_- + \lambda_5)r_\Delta^2)}$	0
$h^2 \bar{\psi}_{L,p} \psi_{R,r}$	$\frac{v_{\text{ew}}c_W(2+(2\lambda_- + \lambda_5)r_\Delta^2)}{\sqrt{2}\epsilon^2\kappa(2-3\kappa+\kappa\lambda_- r_\Delta^2)} Y_\psi^{pr}$	$\frac{3\tilde{\epsilon}^2(1+2\lambda_- \tilde{r}_\Delta^2)}{\sqrt{2}\tilde{v}_{\text{ew}}} Y_\psi^{pr}$
$W_\mu^- W^{+\mu} \bar{\psi}_{L,p} \psi_{R,r}$	$-\frac{v_{\text{ew}}(1+\lambda_- r_\Delta^2)}{\sqrt{2}\epsilon^2 g^2 r_\Delta^2 \kappa(1-\kappa)} Y_\psi^{pr}$	0
$Z_\mu Z^\mu \bar{\psi}_{L,p} \psi_{R,r}$	$-\frac{\sqrt{2}\epsilon^2 g^2(2-\kappa)\kappa r_\Delta^2}{2v_{\text{ew}}c_W^2(1+\lambda_- r_\Delta^2)} Y_\psi^{pr}$	0
$\Delta L = 2$		
$h^2 (\overline{\nu_{L,p}^c} \nu_{L,r})$	$\frac{\epsilon(2-3\kappa+\kappa\lambda_- r_\Delta^2)}{2v_{\text{ew}}(1+\lambda_- r_\Delta^2)} Y_\Delta^{pr}$	$-\frac{\tilde{\epsilon}}{2\tilde{v}_{\text{ew}}}(1+\lambda_- \tilde{r}_\Delta^2) Y_\Delta^{pr}$
$W_\mu^- W^{+\mu} (\overline{\nu_{L,p}^c} \nu_{L,r})$	$-\frac{\epsilon g^2 r_\Delta^2(1-\kappa)}{2v_{\text{ew}}(1+2\lambda_- r_\Delta^2)} Y_\Delta^{pr}$	0
$W_\mu^+ W^{+\mu} (\overline{e_{L,p}^c} e_{L,r})$	$-\frac{\epsilon g^2 r_\Delta^2}{2v_{\text{ew}}(1+(\lambda_- + \lambda_5)r_\Delta^2)} Y_\Delta^{pr}$	0
$W_\mu^+ Z^\mu (\overline{\nu_{L,p}^c} e_{L,r})$	$-\frac{\sqrt{2}\epsilon g^2 r_\Delta^2}{v_{\text{ew}}c_W(2+(2\lambda_- + \lambda_5)r_\Delta^2)} Y_\Delta^{pr}$	0
$Z_\mu Z^\mu (\overline{\nu_{L,p}^c} \nu_{L,r})$	$-\frac{\epsilon g^2 r_\Delta^2(2-\kappa)}{2v_{\text{ew}}c_W^2(1+2\lambda_- r_\Delta^2)} Y_\Delta^{pr}$	0

**Table 3.** WCs for the dim-5 operators in the bEFT and bSMEFT.

## 6 Numerical evaluation

To assess how well the bEFT and bSMEFT frameworks reproduce the results of the UV theory, we calculate the cross sections for two typical processes involving the Higgs boson: one is the subprocess of Higgs pair production via vector boson fusion at the LHC, and the other is the Higgsstrahlung process at a future electron-positron collider. To calculate the

dim-6 with $\Delta L = 0$			
Notation	Operator	WC in bEFT	WC in bSMEFT
$\mathcal{O}_{(\partial h)^2 W^2}$	$(\partial_\mu h)(\partial_\nu h)W^{-\mu}W^{+\nu}$	$\frac{4\epsilon^2 g^2 r_\Delta^2 (1-2\kappa)^2}{v_{\text{ew}}^2 (2 + (2\lambda_- + \lambda_5)r_\Delta^2)}$	0
$\mathcal{O}_{h^2(\partial W)^2}$	$hh(D_\mu W^{-\mu})(D_\nu W^{+\nu})$	$-\frac{\epsilon^2 g^2 r_\Delta^2 (1-2\kappa)^2}{v_{\text{ew}}^2 (2 + (2\lambda_- + \lambda_5)r_\Delta^2)}$	0
$\mathcal{O}_{h^2\partial^2 WW}$	$hh(D_\mu D_\nu W^{-\mu})W^{+\nu}$	$-\frac{\epsilon^2 g^2 r_\Delta^2 (1-2\kappa)^2}{v_{\text{ew}}^2 (2 + (2\lambda_- + \lambda_5)r_\Delta^2)}$	0
$\mathcal{O}_{(\partial h)^2 Z^2}$	$(\partial_\mu h)(\partial_\nu h)Z^\mu Z^\nu$	$\frac{2\epsilon^2 g^2 r_\Delta^2 (1-2\kappa)^2}{v_{\text{ew}}^2 c_W^2 (1 + \lambda_- r_\Delta^2)}$	0
$\mathcal{O}_{h^2(\partial Z)^2}$	$hh(\partial_\mu Z^\mu)(\partial_\nu Z^\nu)$	$-\frac{\epsilon^2 g^2 r_\Delta^2 (1-2\kappa)^2}{2v_{\text{ew}}^2 c_W^2 (1 + \lambda_- r_\Delta^2)}$	0
$\mathcal{O}_{h^2\partial^2 ZZ}$	$hhZ^\mu(\partial_\nu\partial_\mu Z^\nu)$	$-\frac{\epsilon^2 g^2 r_\Delta^2 (1-2\kappa)^2}{v_{\text{ew}}^2 c_W^2 (1 + \lambda_- r_\Delta^2)}$	0
$\mathcal{O}_{(\partial h)Zee}$	$i(\partial_\mu h)Z^\mu(\bar{e}_R^p e_L^r)$	$-\frac{2\sqrt{2}\epsilon^2 g r_\Delta^2 (2\kappa-1)}{v_{\text{ew}}^2 c_W (1 + \lambda_- r_\Delta^2)}$	0
$\mathcal{O}_{h(\partial Z)ee}$	$ih(\partial_\mu Z^\mu)(\bar{e}_R^p e_L^r)$	$-\frac{\sqrt{2}\epsilon^2 g r_\Delta^2 (2\kappa-1)}{v_{\text{ew}}^2 c_W (1 + \lambda_- r_\Delta^2)}$	0

**Table 4.** WCs for the dim-6 operators in the bEFT and bSMEFT.

scattering amplitude squared, we employ the Mathematica package `FeynCalc` [55, 56]. The original free parameters in the scalar potential are  $m_H$ ,  $\lambda$ ,  $M_\Delta$ ,  $\Lambda_6$ , and  $\lambda_i$  ( $i = 1, 2, 4, 5$ ). After imposing minimization conditions, our input parameters are chosen as  $\lambda$ ,  $r_\Delta$ ,  $\epsilon$ ,  $v_{\text{ew}}$ ,  $\lambda_-$ , and  $\lambda_i$  ( $i = 1, 2, 5$ ). We set the scalar couplings  $\lambda_1 = \lambda_2 = \lambda_5 = 1$  while varying the value of  $\lambda_-$ . We checked that within the parameter region we focus on, the Higgs cubic,  $hWW$ , and  $hZZ$  couplings satisfy the current LHC constraints,  $-0.4 < \kappa_\lambda < 6.3$  [57],  $-0.06 \leq \Delta\kappa_W \leq 0.10$ , and  $-0.03 \leq \Delta\kappa_Z \leq 0.11$  [58], respectively. We assume the maximal value of  $v_\Delta \simeq 1$  GeV that is allowed by the  $\rho$  parameter, which implies  $\epsilon \simeq 10^{-2}$ . In this case, the doubly charged Higgs bosons  $H^{\pm\pm}$  decay mainly into a pair of like-charge  $W^\pm$  bosons, and the lower bound on their mass is relatively relaxed,  $m_{H^{\pm\pm}} \gtrsim 400$  GeV [59, 60].

In Fig. 1, we show the cross section of  $W^-W^+ \rightarrow hh$  in each theory at a center-of-mass energy  $\sqrt{s} = 400$  GeV with a fixed value of  $\epsilon = 10^{-2}$ . We assume  $\lambda_- = 0.5, 3$ , and  $5$  in the top, middle, and bottom panels, respectively. In the left panels, the green solid, red dashed, and blue dotted curves correspond to the results in the UV theory, bEFT, and bSMEFT, while the gray solid line denotes the SM value. In the right panels, we plot the relative deviations of cross sections in the bEFT and the bSMEFT from that in the UV. The upper horizontal axis in each plot gives the ratio of the center of mass energy to the

mass of the lightest new scalar. As can be seen from the figure, the bEFT reproduces very well the result of the UV theory in the whole range of the parameters shown. In contrast, the bSMEFT result deviates much more significantly from the UV result, and the deviation flips sign with the increase of  $\lambda_-$ . As can be seen from the figure, even when we take the limit of  $r_\Delta \rightarrow 0$ , or equivalently,  $M_\Delta \rightarrow \infty$ , the UV and EFT cross sections still deviate from the SM value, indicating that the new physics effect does not decouple. This can be understood as follows: since we fix the  $\epsilon$  to a finite value, the triplet VEV remains nonzero and it induces the new physics effect through  $\lambda_{4,5}$  and  $\Lambda_6$  interactions in Eq. (2.3).

In Fig. 2 the same cross section is plotted as a function of  $\epsilon$  at the fixed  $r_\Delta = 0.4$ , using the same legends as in Fig. 1. Note that the masses of the heavy scalars vary with our input parameters. For instance, if we take the value of  $\epsilon$  as  $\epsilon = 10^{-2}$ , the masses of the heavy scalars are respectively,  $(M_{H_0}, M_{A_0}, M_{H^\pm}, M_{H^{\pm\pm}})/\text{GeV} = (640, 640, 663, 685)$  at  $\lambda_- = 0.5$ ,  $(749, 749, 769, 788)$  at  $\lambda_- = 3$ , and  $(826, 826, 844, 862)$  at  $\lambda_- = 5$ . Again the bEFT result is precise at the per mille level or better while the bSMEFT deviates significantly from the UV theory for a slightly larger value of  $\epsilon$ . As can be seen from the figure, when we take the limit of  $\epsilon \rightarrow 0$  while fixing  $r_\Delta = 0.4$ , the UV and EFT cross sections converge to the SM value. This reflects the following fact: the limit  $\epsilon \rightarrow 0$  corresponds to the vanishing VEV of the scalar triplet, so it is equivalent to the limit of  $\Lambda_6 \rightarrow 0$ . In this limit, the scalar triplet interacts with the Higgs doublet only in pairs in Eq. (2.3), so it does not affect  $W^-W^+ \rightarrow hh$  at tree level. Fig. 3 and Fig. 4 show the corresponding results for the process  $e^+e^- \rightarrow Zh$  at  $\sqrt{s} = 250$  GeV. The conclusion is the same as for the  $W^-W^+ \rightarrow hh$  process, with the main difference being that the bSMEFT result is constantly larger than the UV result.

The reason why the bEFT reproduces the results of the UV theory better than the bSMEFT is due to the difference in power counting between the two EFTs. We demonstrate this using the process  $W^-(p_1)W^+(p_2) \rightarrow h(p_3)h(p_4)$  as an example. As can be seen in Table 4, the bEFT has dim-6 operators that contribute to  $W^-W^+ \rightarrow hh$ , while the bSMEFT does not. This is because in the bSMEFT, effective operators with derivatives that give corrections to  $W^-W^+ \rightarrow hh$ , such as  $((D_\mu H)^\dagger D_\mu H)^2$ , only appear at the dim-8 level or higher. This makes the bSMEFT less accurate in reproducing the UV results, as we show below.

In the UV theory, the contribution to  $W^-W^+ \rightarrow hh$  is given by

$$\mathcal{M}^{\text{UV}} = \mathcal{M}_h^{\text{UV}} + \mathcal{M}_{W^\pm}^{\text{UV}} + \mathcal{M}_{H_0}^{\text{UV}} + \mathcal{M}_{H^\pm}^{\text{UV}} + \mathcal{M}_{\text{contact}}^{\text{UV}}. \quad (6.1)$$

The terms  $\mathcal{M}_{h,H_0}^{\text{UV}}$  are the  $s$ -channel amplitudes mediated by  $h$ ,  $H_0$ , and the terms  $\mathcal{M}_{W^\pm, H^\pm}^{\text{UV}}$  are the  $t, u$ -channel amplitudes mediated by  $W^\pm$ ,  $H^\pm$ , respectively. The term  $\mathcal{M}_{\text{contact}}^{\text{UV}}$  is from the contact interaction. In both EFTs, the contributions mediated by  $H_0, H^\pm$  are incorporated into the contact part. Note that  $\mathcal{M}_{h,W^\pm}^{\text{UV}}$  and  $\mathcal{M}_{\text{contact}}^{\text{UV}}$  are different from their counterparts in the SM since the  $hW^2$  and  $h^2W^2$  couplings deviate from the SM through

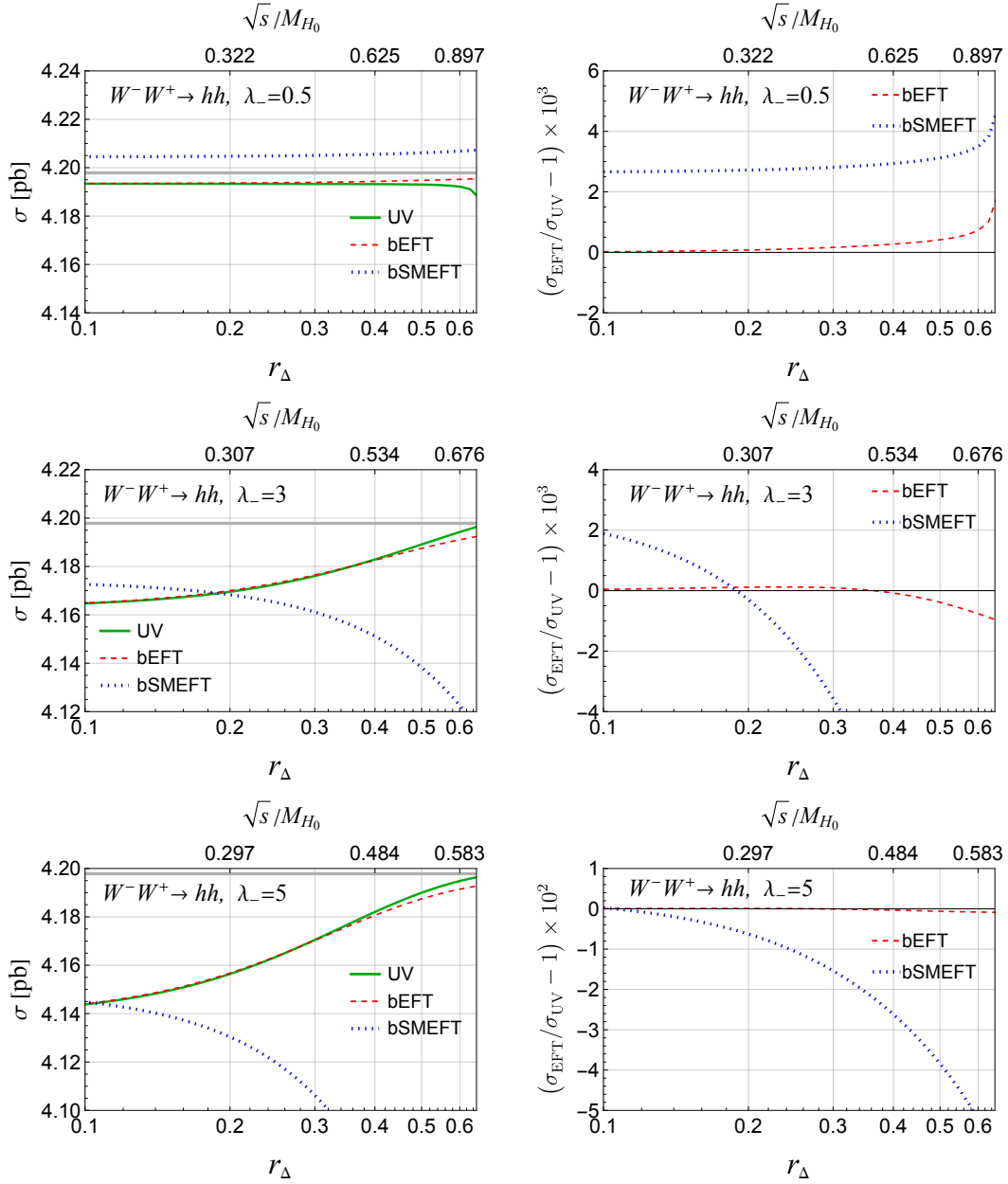


**Figure 1.** Comparison of cross sections for  $W^+W^- \rightarrow hh$  as a function of  $r_\Delta$  or  $\sqrt{s}/M_{H_0}$  calculated in the three theories at the fixed  $\epsilon = 10^{-2}$ . The gray solid line on the left panels denotes the SM value.

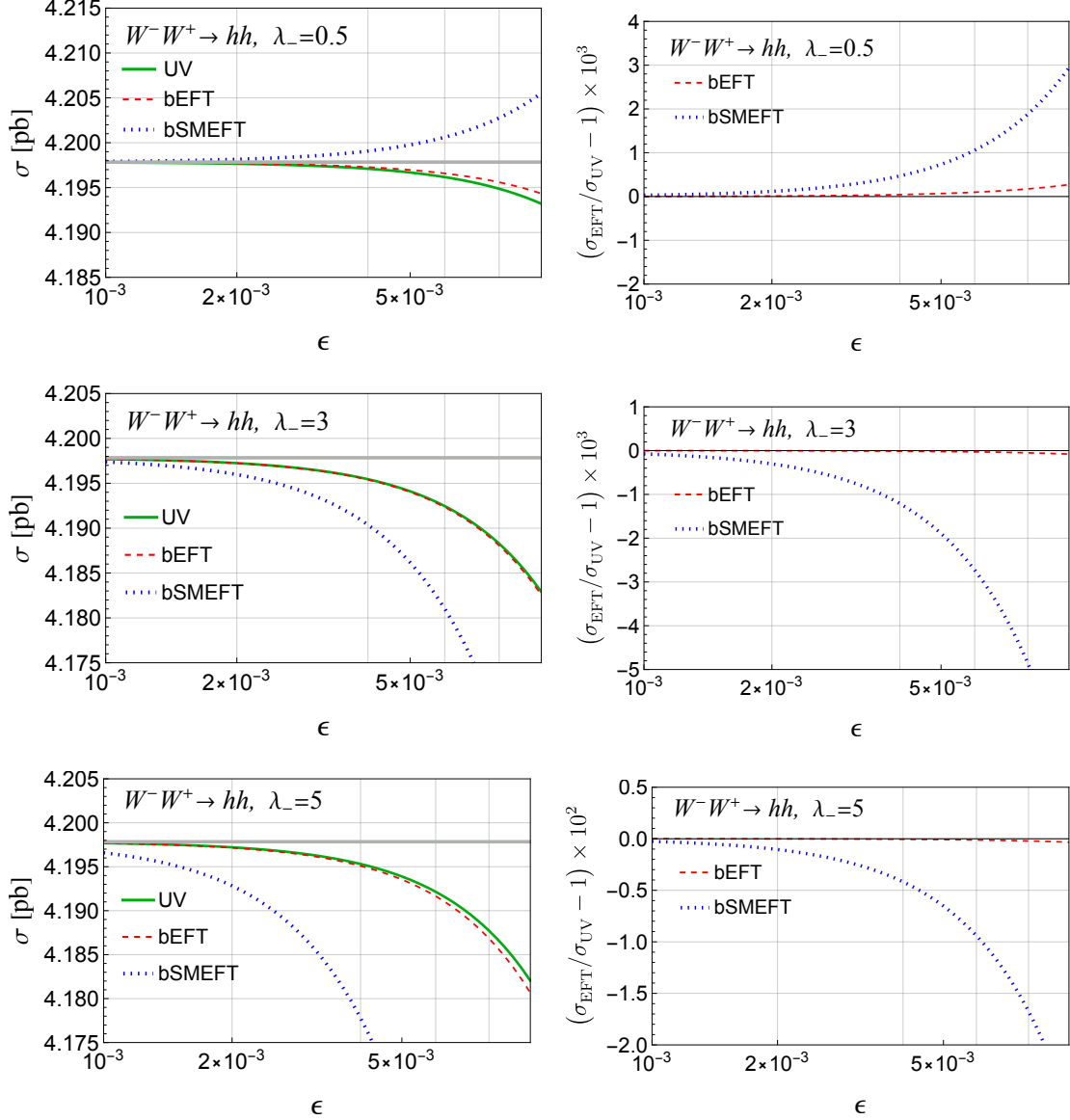


**Figure 2.** Comparison of cross sections for  $W^+W^- \rightarrow hh$  as a function of  $\epsilon$  calculated in the three theories at the fixed  $r_\Delta = 0.4$ . The gray solid line on the left panels denotes the SM value.

the scalar mixing. Below we will show that the UV amplitude (6.1) coincides with the amplitude in the bEFT up to order  $\epsilon^2$  if we take the limit of  $s$ ,  $|t|$ ,  $|u| \ll M_\Delta^2$ , where  $s = (p_1 + p_2)^2$ ,  $t = (p_1 - p_3)^2$ , and  $u = (p_1 - p_4)^2$ .

First of all, since the  $h^3$  and  $hW^2$  couplings in the UV theory coincide with those in the bEFT as we have emphasized in Section 5, the bEFT exactly reproduces the contributions

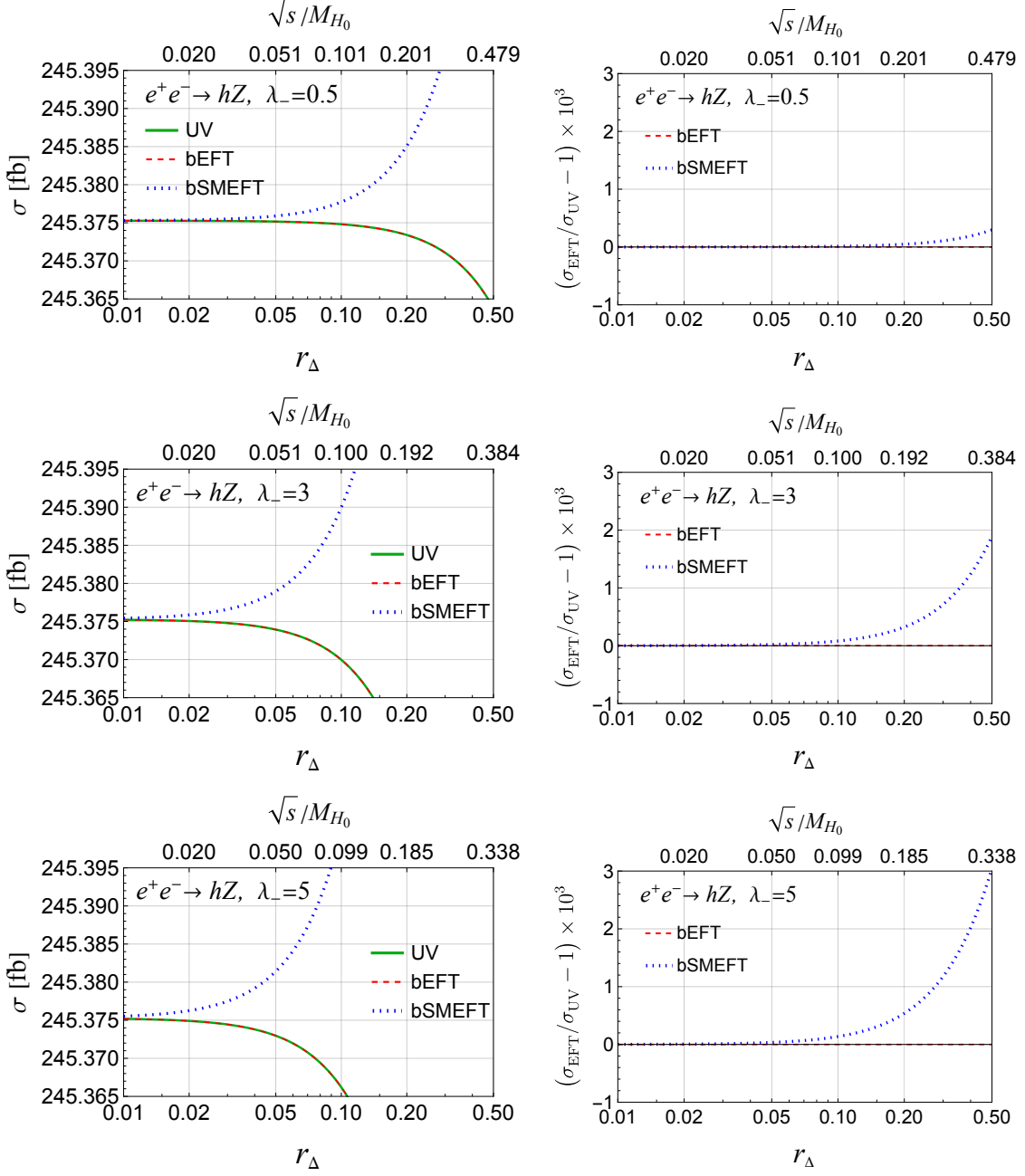


**Figure 3.** Same as Fig. 1 but for the process  $e^+e^- \rightarrow hZ$ .

$\mathcal{M}_{h,W^\pm}^{\text{UV}}$ . Consider next the contribution associated with  $\mathcal{M}_{H^\pm}^{\text{UV}}$ . In the UV theory, it is

$$\mathcal{M}_{H^\pm}^{\text{UV}} = -(C_{hHW}^{\text{UV}})^2 \left( \frac{(2p_3 - p_1)_\mu (2p_4 - p_2)_\nu}{t - m_{H^\pm}^2} + \frac{(2p_4 - p_1)_\mu (2p_3 - p_2)_\nu}{u - m_{H^\pm}^2} \right) \epsilon^\mu(p_1) \epsilon^\nu(p_2), \quad (6.2)$$

where  $\epsilon^\mu(p_i)$  is the polarization vector for the  $W$  boson with momentum  $p_i$ . In the bEFT, on the other hand, it is replaced by the contact interactions  $\mathcal{O}_{(\partial h)^2 W^2}$ ,  $\mathcal{O}_{h^2 (\partial W)^2}$ , and

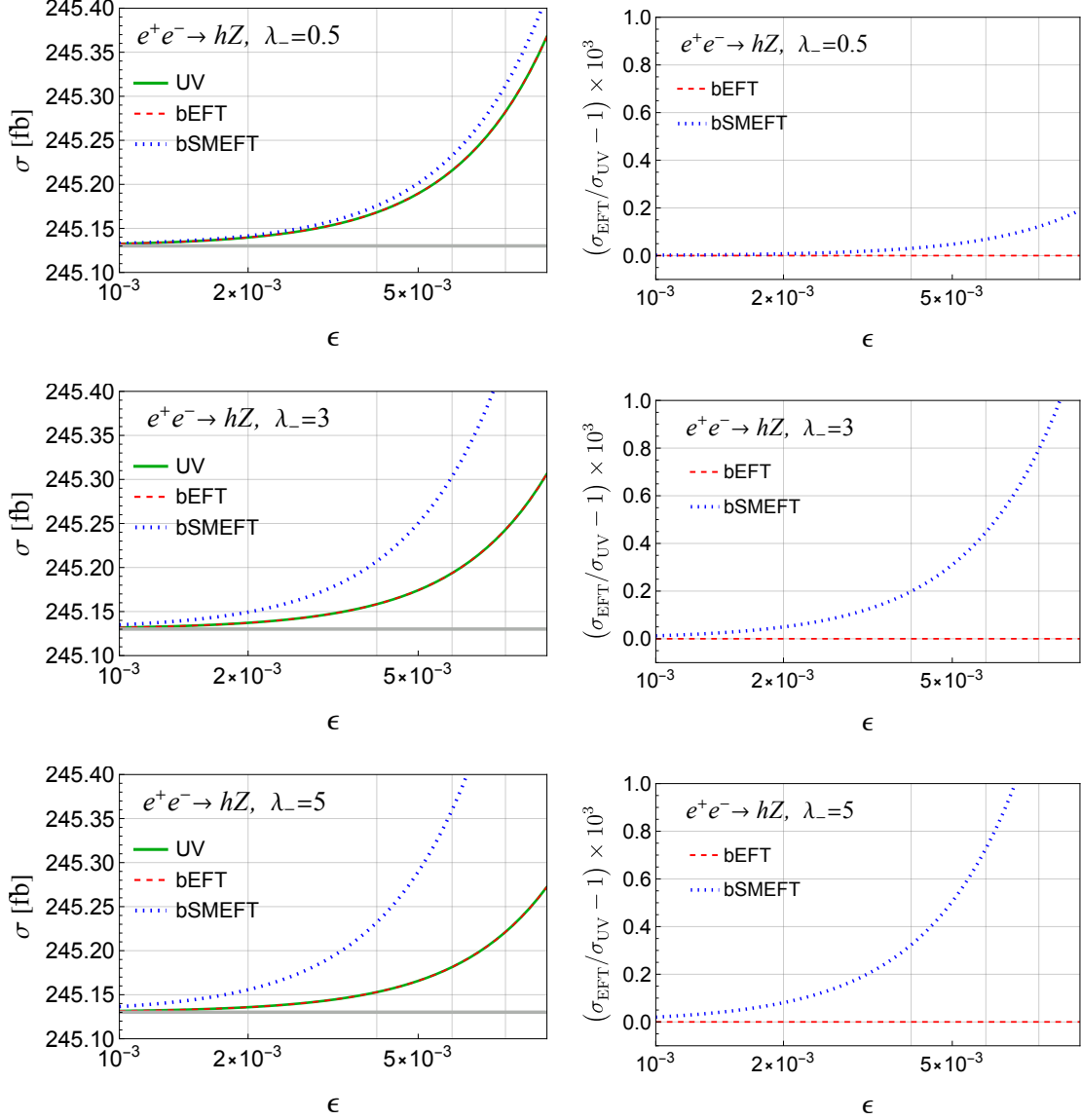


**Figure 4.** Same as Fig. 2 but for the process  $e^+e^- \rightarrow hZ$ .

$\mathcal{O}_{h^2\partial^2 WW}$ , resulting in

$$\mathcal{M}_{\text{dim-6}}^{\text{bEFT}} = \frac{\epsilon^2 g^2 r_\Delta^2 (1 - 2\kappa)^2}{v_{\text{ew}}^2 (2 + r_\Delta^2 \lambda_4)} \left[ (2p_3 - p_1)_\mu (2p_4 - p_2)_\nu + (2p_4 - p_1)_\mu (2p_3 - p_2)_\nu \right] \epsilon^\mu(p_1) \epsilon^\nu(p_2). \quad (6.3)$$

Eq. (6.2) coincides with Eq. (6.3) up to order  $\epsilon^2$  in the limit of  $|t|, |u| \ll m_{H^\pm}^2$  by the relation,

$$\frac{(C_{hHW}^{\text{UV}})^2}{m_{H^\pm}^2} = \frac{\epsilon^2 g^2 r_\Delta^2 (1 - 2\kappa)^2}{v_{\text{ew}}^2 (2 + r_\Delta^2 \lambda_4)} + \mathcal{O}(\epsilon^4). \quad (6.4)$$

Lastly, we show how the bEFT reproduces  $\mathcal{M}_{H_0}^{\text{UV}}$  and  $\mathcal{M}_{\text{contact}}^{\text{UV}}$ . Their explicit forms are given by

$$\mathcal{M}_{H_0}^{\text{UV}} = -C_{h^2 H_0}^{\text{UV}} C_{H_0 W^2}^{\text{UV}} \frac{1}{s - M_{H_0}^2}, \quad (6.5a)$$

$$\mathcal{M}_{\text{contact}}^{\text{UV}} = C_{h^2 W^2}^{\text{UV}}. \quad (6.5b)$$

In the bEFT, they are replaced by the contact interaction  $h^2 W_\mu^- W^{+\mu}$  given in Table 2:

$$\mathcal{M}_{\text{dim-4}}^{\text{bEFT}} = \frac{g^2}{4} \left[ 1 - \epsilon^2 \frac{4(1 - 2\kappa)(2 - \kappa + \kappa\lambda_- r_\Delta^2)}{1 + \lambda_- r_\Delta^2} \right]. \quad (6.6)$$

It is easy to see that the sum of  $\mathcal{M}_{H_0}^{\text{UV}}$  and  $\mathcal{M}_{\text{contact}}^{\text{UV}}$  coincides with Eq. (6.6) up to order  $\epsilon^2$  in the limit of  $s \ll m_{H_0}^2$  by applying the relation,

$$\frac{C_{h^2 H_0}^{\text{UV}} C_{H_0 W^2}^{\text{UV}}}{M_{H_0}^2} + C_{h^2 W^2}^{\text{UV}} = \mathcal{M}_{\text{dim-4}}^{\text{bEFT}} + \mathcal{O}(\epsilon^4). \quad (6.7)$$

To summarize, the UV amplitude (6.1) coincides with the amplitude in the bEFT up to order  $\epsilon^2$  in the low energy limit of  $s$ ,  $|t|$ ,  $|u| \ll M_\Delta^2$ .

In the bSMEFT, the heavy fields are integrated out before the electroweak symmetry breaking. The drawback with this is that the bSMEFT does not properly take into account the effects of the scalar mixing in the broken phase unless we work to a higher order in power counting. For example, the coupling  $C_{hHW}^{\text{UV}}$  appearing in  $\mathcal{M}_{H^\pm}^{\text{UV}}$  is generated by the mixing between the charged components in the  $\text{SU}(2)_L$  doublet  $H$  and triplet  $\Delta$ . In the bEFT, the scalar mixing is incorporated at the very start, so the contribution of Eq. (6.3) arises from the dim-6 operators and reproduces  $\mathcal{M}_{H^\pm}^{\text{UV}}$  in the low energy limit. In contrast, there is no contact interaction with derivatives in the bSMEFT up to the dim-6 level that contributes to  $W^- W^+ \rightarrow hh$ , as can be seen in Table 4. Although the bSMEFT has an  $h^2 W^2$  operator as shown in Table 2, this operator does not involve derivatives and therefore is not enough to describe accurately the momentum dependence of processes mediated by  $H^\pm$ . As a matter of fact, the bSMEFT treats the  $H_0$ ,  $A_0$ ,  $H^\pm$ , and  $H^{\pm\pm}$  together as a single triplet field. This means it makes not much sense to speak of their separate contributions at the leading low energy order. Now the reason becomes clear why the bEFT reproduces the low energy result of the UV theory more accurately than the bSMEFT: it comes from the difference in power counting. The bEFT incorporates the effects of scalar mixing at low orders of the perturbative expansion, while the bSMEFT cannot unless it is expanded to higher orders. Therefore the bEFT can be considered as a better organization of low energy expansion of the UV theory.

## 7 Conclusion

In this work we have introduced the broken phase EFT (bEFT) whose symmetry is  $\text{SU}(3)_c \times \text{U}(1)_{\text{em}}$  and degrees of freedom are the SM particles in the broken phase. We considered the

matching of the type-II seesaw model onto the bEFT at tree level up to dim-6 operators. To make comparisons with the SMEFT, we rewrote the results of matching the type-II seesaw model onto the SMEFT in a basis after the symmetry breaking, named as bSMEFT. To compare the two EFTs concretely, we evaluated the Higgs pair production through vector-boson fusion and the single Higgs production through the Higgsstrahlung process using the type-II seesaw, bEFT, and bSMEFT. We found that the bEFT generically reproduces the results of the type-II seesaw model more accurately than the bSMEFT. The difference arises from power counting, i.e., the organization of perturbative expansion. In the bSMEFT, the heavy fields are integrated out before electroweak symmetry breaking, so that the effect of mixing between the scalar fields is not incorporated at the leading order. In the bEFT, on the other hand, the heavy fields are integrated out after electroweak symmetry breaking whence their mixing with the light scalar has been taken into account. This is in accord with the physical intuition that the SMEFT may not work well when new heavy scalars participate in the electroweak symmetry breaking or when new particles are not heavy enough compared with the electroweak scale. In the future work, we will apply the bEFT to the cases when the SM gauge symmetry is extended, such as the Grand Unified Theory and the left-right symmetric model.

## Acknowledgements

YU would like to thank Masaharu Tanabashi and Koji Tsumura for the fruitful discussion. This work was supported in part by the Grants No. NSFC-12035008, No. NSFC-12305110, and No. NSFC-12347112, and by the Guangdong Major Project of Basic and Applied Basic Research No. 2020B0301030008.

## A Minimization of the scalar potential

We derive the minimization condition of the scalar potential in Eq. (2.3) and the mass eigenstates of the scalar fields after symmetry breaking. Substituting the VEVs of the  $SU(2)_L$  doublet and triplet scalar fields denoted by  $\langle H \rangle$  and  $\langle \Delta \rangle$  into the scalar potential, we get

$$\mathcal{V}(\langle H \rangle, \langle \Delta \rangle) = \frac{1}{2}M_\Delta^2 v_\Delta^2 + \frac{1}{8}\lambda v_H^4 + \frac{1}{8}\lambda_1 v_\Delta^4 + \frac{1}{2}\lambda_- v_H^2 v_\Delta^2 - \frac{1}{2}\Lambda_6 v_H^2 v_\Delta - \frac{1}{2}m_H^2 v_H^2. \quad (\text{A.1})$$

Note that  $v_H$  and  $v_\Delta$  satisfy the following relation,

$$v_{\text{ew}} = \sqrt{v_H^2 + 2v_\Delta^2}, \quad (\text{A.2})$$

with  $v_{\text{ew}} = 246$  GeV. The conditions for the scalar potential to take an extreme value at  $v_H$  and  $v_\Delta$  are

$$\frac{\partial \mathcal{V}(\langle H \rangle, \langle \Delta \rangle)}{\partial v_H} = v_H \left( \frac{1}{2}\lambda v_H^2 - \Lambda_6 v_\Delta + \lambda_- v_\Delta^2 - m_H^2 \right) = 0, \quad (\text{A.3a})$$

$$\frac{\partial \mathcal{V}(\langle H \rangle, \langle \Delta \rangle)}{\partial v_\Delta} = v_\Delta \left( -\frac{1}{2} \frac{\Lambda_6 v_H^2}{v_\Delta} + \lambda_- v_H^2 + \frac{1}{2} \lambda_1 v_\Delta^2 + M_\Delta^2 \right) = 0. \quad (\text{A.3b})$$

Solving the above, we get

$$m_H^2 = \frac{1}{2} \lambda v_H^2 - \Lambda_6 v_\Delta + \lambda_- v_\Delta^2, \quad (\text{A.4a})$$

$$M_\Delta^2 = \frac{1}{2} \frac{\Lambda_6 v_H^2}{v_\Delta} - \lambda_- v_H^2 - \frac{1}{2} \lambda_1 v_\Delta^2. \quad (\text{A.4b})$$

We replace the original parameters  $m_H^2$  and  $\Lambda_6$  with the two VEVs by using the above two relations. The mass terms for the scalar fields are given by

$$\begin{aligned} -\mathcal{L}_{\text{mass}} = & \frac{1}{2} (h, \delta^0) \mathcal{M}_{\text{CPeven}}^2 \begin{pmatrix} h \\ \delta^0 \end{pmatrix} + \frac{1}{2} (\chi, \eta) \mathcal{M}_{\text{CPodd}}^2 \begin{pmatrix} \chi \\ \eta \end{pmatrix} \\ & + (H^-, \delta^-) \mathcal{M}_{\text{Charged}}^2 \begin{pmatrix} H^+ \\ \delta^+ \end{pmatrix} + m_{H^{\pm\pm}}^2 H^{--} H^{++}, \end{aligned} \quad (\text{A.5})$$

where the explicit forms of mass matrices are

$$\mathcal{M}_{\text{CPeven}}^2 = \begin{pmatrix} \lambda v^2 & -\frac{v_\Delta}{v} (2M_\Delta^2 + \lambda_1 v_\Delta^2) \\ -\frac{v_\Delta}{v} (2M_\Delta^2 + \lambda_1 v_\Delta^2) & M_\Delta^2 + \frac{3}{2} \lambda_1 v_\Delta^2 + \lambda_- v^2 \end{pmatrix}, \quad (\text{A.6a})$$

$$\mathcal{M}_{\text{CPodd}}^2 = \frac{2M_\Delta^2 + \lambda_1 v_\Delta^2 + 2\lambda_- v^2}{2v^2} \begin{pmatrix} 4v_\Delta^2 & -2vv_\Delta \\ -2vv_\Delta & v^2 \end{pmatrix}, \quad (\text{A.6b})$$

$$\mathcal{M}_{\text{Charged}}^2 = \frac{2M_\Delta^2 + \lambda_1 v_\Delta^2 + \lambda_4 v^2}{2v^2} \begin{pmatrix} 2v_\Delta^2 & -\sqrt{2}vv_\Delta \\ -\sqrt{2}vv_\Delta & v^2 \end{pmatrix}. \quad (\text{A.6c})$$

By diagonalizing the above mass matrices, we obtain the masses for the scalar fields as

$$m_{H^{\pm\pm}}^2 = M_\Delta^2 + (\lambda_- + \lambda_5) v^2 + \frac{1}{2} (\lambda_1 + \lambda_2) v_\Delta^2, \quad (\text{A.7a})$$

$$m_{H^\pm}^2 = \left( M_\Delta^2 + \frac{1}{2} \lambda_4 v^2 + \frac{1}{2} \lambda_1 v_\Delta^2 \right) \left( 1 + \frac{2v_\Delta^2}{v^2} \right), \quad (\text{A.7b})$$

$$m_{A_0}^2 = \left( M_\Delta^2 + \lambda_- v^2 + \frac{1}{2} \lambda_1 v_\Delta^2 \right) \left( 1 + \frac{4v_\Delta^2}{v^2} \right), \quad (\text{A.7c})$$

$$m_h^2 = \frac{1}{2} \left( A + C - \sqrt{(A - C)^2 + 4B^2} \right), \quad (\text{A.7d})$$

$$m_{H_0}^2 = \frac{1}{2} \left( A + C + \sqrt{(A - C)^2 + 4B^2} \right), \quad (\text{A.7e})$$

where  $A$ ,  $B$ , and  $C$  are given by

$$A = \lambda v^2, \quad (\text{A.8a})$$

$$B = -\frac{2v_\Delta}{v} \left( M_\Delta^2 + \frac{1}{2} \lambda_1 v_\Delta^2 \right), \quad (\text{A.8b})$$

$$C = M_\Delta^2 + \lambda_- v^2 + \frac{3}{2} \lambda_1 v_\Delta^2. \quad (\text{A.8c})$$

## References

- [1] **ATLAS** Collaboration, “Observation of a new particle in the search for the Standard Model Higgs boson with the ATLAS detector at the LHC,” *Phys. Lett. B* **716** (2012) 1–29 [[arXiv:1207.7214](#)].
- [2] **CMS** Collaboration, “Observation of a New Boson at a Mass of 125 GeV with the CMS Experiment at the LHC,” *Phys. Lett. B* **716** (2012) 30–61 [[arXiv:1207.7235](#)].
- [3] P. Minkowski, “ $\mu \rightarrow e\gamma$  at a Rate of One Out of  $10^9$  Muon Decays?” *Phys. Lett. B* **67** (1977) 421–428.
- [4] O. Sawada and A. Sugamoto, eds., “Horizontal gauge symmetry and masses of neutrinos,” *Conf. Proc. C* **7902131** (1979) 95–99.
- [5] M. Gell-Mann, P. Ramond, and R. Slansky, “Complex Spinors and Unified Theories,” *Conf. Proc. C* **790927** (1979) 315–321 [[arXiv:1306.4669](#)].
- [6] S. L. Glashow, “The Future of Elementary Particle Physics,” *NATO Sci. Ser. B* **61** (1980) 687.
- [7] R. N. Mohapatra and G. Senjanovic, “Neutrino Mass and Spontaneous Parity Nonconservation,” *Phys. Rev. Lett.* **44** (1980) 912.
- [8] R. E. Shrock, “General Theory of Weak Leptonic and Semileptonic Decays. 1. Leptonic Pseudoscalar Meson Decays, with Associated Tests For, and Bounds on, Neutrino Masses and Lepton Mixing,” *Phys. Rev. D* **24** (1981) 1232.
- [9] J. Schechter and J. W. F. Valle, “Neutrino Masses in  $SU(2) \times U(1)$  Theories,” *Phys. Rev. D* **22** (1980) 2227.
- [10] W. Konetschny and W. Kummer, “Nonconservation of Total Lepton Number with Scalar Bosons,” *Phys. Lett. B* **70** (1977) 433–435.
- [11] M. Magg and C. Wetterich, “Neutrino Mass Problem and Gauge Hierarchy,” *Phys. Lett. B* **94** (1980) 61–64.
- [12] T. P. Cheng and L.-F. Li, “Neutrino Masses, Mixings and Oscillations in  $SU(2) \times U(1)$  Models of Electroweak Interactions,” *Phys. Rev. D* **22** (1980) 2860.
- [13] R. N. Mohapatra and G. Senjanovic, “Neutrino Masses and Mixings in Gauge Models with Spontaneous Parity Violation,” *Phys. Rev. D* **23** (1981) 165.
- [14] G. Lazarides, Q. Shafi, and C. Wetterich, “Proton Lifetime and Fermion Masses in an  $SO(10)$  Model,” *Nucl. Phys. B* **181** (1981) 287–300.
- [15] R. Foot, H. Lew, X. G. He, and G. C. Joshi, “Seesaw Neutrino Masses Induced by a Triplet of Leptons,” *Z. Phys. C* **44** (1989) 441.
- [16] Z.-j. Tao, “Radiative seesaw mechanism at weak scale,” *Phys. Rev. D* **54** (1996) 5693–5697 [[hep-ph/9603309](#)].
- [17] E. Ma, “Verifiable radiative seesaw mechanism of neutrino mass and dark matter,” *Phys. Rev. D* **73** (2006) 077301 [[hep-ph/0601225](#)].

- [18] Y. Cai, J. Herrero-García, M. A. Schmidt, A. Vicente, and R. R. Volkas, “From the trees to the forest: a review of radiative neutrino mass models,” *Front. in Phys.* **5** (2017) 63 [[arXiv:1706.08524](#)].
- [19] S. Weinberg, “Baryon and Lepton Nonconserving Processes,” *Phys. Rev. Lett.* **43** (1979) 1566–1570.
- [20] W. Buchmuller and D. Wyler, “Effective Lagrangian Analysis of New Interactions and Flavor Conservation,” *Nucl. Phys. B* **268** (1986) 621–653.
- [21] C. N. Leung, S. T. Love, and S. Rao, “Low-Energy Manifestations of a New Interaction Scale: Operator Analysis,” *Z. Phys. C* **31** (1986) 433.
- [22] B. Grzadkowski, M. Iskrzynski, M. Misiak, and J. Rosiek, “Dimension-Six Terms in the Standard Model Lagrangian,” *JHEP* **10** (2010) 085 [[arXiv:1008.4884](#)].
- [23] F. Feruglio, “The Chiral approach to the electroweak interactions,” *Int. J. Mod. Phys. A* **8** (1993) 4937–4972 [[hep-ph/9301281](#)].
- [24] J. Bagger, *et al.*, “The Strongly interacting W W system: Gold plated modes,” *Phys. Rev. D* **49** (1994) 1246–1264 [[hep-ph/9306256](#)].
- [25] V. Koulovassilopoulos and R. S. Chivukula, “The Phenomenology of a nonstandard Higgs boson in W(L) W(L) scattering,” *Phys. Rev. D* **50** (1994) 3218–3234 [[hep-ph/9312317](#)].
- [26] C. P. Burgess, J. Matias, and M. Pospelov, “A Higgs or not a Higgs? What to do if you discover a new scalar particle,” *Int. J. Mod. Phys. A* **17** (2002) 1841–1918 [[hep-ph/9912459](#)].
- [27] B. Grinstein and M. Trott, “A Higgs-Higgs bound state due to new physics at a TeV,” *Phys. Rev. D* **76** (2007) 073002 [[arXiv:0704.1505](#)].
- [28] R. Alonso, M. B. Gavela, L. Merlo, S. Rigolin, and J. Yepes, “The Effective Chiral Lagrangian for a Light Dynamical ”Higgs Particle”,” *Phys. Lett. B* **722** (2013) 330–335 [[arXiv:1212.3305](#)]. [Erratum: *Phys.Lett.B* 726, 926 (2013)].
- [29] D. Espriu, F. Mescia, and B. Yengo, “Radiative corrections to WL WL scattering in composite Higgs models,” *Phys. Rev. D* **88** (2013) 055002 [[arXiv:1307.2400](#)].
- [30] G. Buchalla, O. Catà, and C. Krause, “Complete Electroweak Chiral Lagrangian with a Light Higgs at NLO,” *Nucl. Phys. B* **880** (2014) 552–573 [[arXiv:1307.5017](#)]. [Erratum: *Nucl.Phys.B* 913, 475–478 (2016)].
- [31] I. Brivio, *et al.*, “Disentangling a dynamical Higgs,” *JHEP* **03** (2014) 024 [[arXiv:1311.1823](#)].
- [32] R. Alonso, E. E. Jenkins, and A. V. Manohar, “A Geometric Formulation of Higgs Effective Field Theory: Measuring the Curvature of Scalar Field Space,” *Phys. Lett. B* **754** (2016) 335–342 [[arXiv:1511.00724](#)].
- [33] R. Alonso, E. E. Jenkins, and A. V. Manohar, “Geometry of the Scalar Sector,” *JHEP* **08** (2016) 101 [[arXiv:1605.03602](#)].
- [34] G. Buchalla, O. Cata, A. Celis, M. Knecht, and C. Krause, “Complete One-Loop

- Renormalization of the Higgs-Electroweak Chiral Lagrangian,” *Nucl. Phys. B* **928** (2018) 93–106 [[arXiv:1710.06412](#)].
- [35] R. Alonso, K. Kanshin, and S. Saa, “Renormalization group evolution of Higgs effective field theory,” *Phys. Rev. D* **97** (2018) 035010 [[arXiv:1710.06848](#)].
- [36] J. de Blas, O. Eberhardt, and C. Krause, “Current and Future Constraints on Higgs Couplings in the Nonlinear Effective Theory,” *JHEP* **07** (2018) 048 [[arXiv:1803.00939](#)].
- [37] A. Falkowski and R. Rattazzi, “Which EFT,” *JHEP* **10** (2019) 255 [[arXiv:1902.05936](#)].
- [38] G. Buchalla, O. Cata, A. Celis, and C. Krause, “Standard Model Extended by a Heavy Singlet: Linear vs. Nonlinear EFT,” *Nucl. Phys. B* **917** (2017) 209–233 [[arXiv:1608.03564](#)].
- [39] S. Dawson, D. Fontes, C. Quezada-Calonge, and J. J. Sanz-Cillero, “Matching the 2HDM to the HEFT and the SMEFT: Decoupling and perturbativity,” *Phys. Rev. D* **108** (2023) 055034 [[arXiv:2305.07689](#)].
- [40] S. Dawson, D. Fontes, C. Quezada-Calonge, and J. J. Sanz-Cillero, “Is the HEFT matching unique?” *Phys. Rev. D* **109** (2024) 055037 [[arXiv:2311.16897](#)].
- [41] G. Buchalla, F. König, C. Müller-Salditt, and F. Pandler, “Two-Higgs Doublet Model Matched to Nonlinear Effective Theory.” [arXiv:2312.13885](#).
- [42] H. Song and X. Wan, “A Non-linear Representation of General Scalar Extensions of the Standard Model for HEFT Matching.” [arXiv:2412.00355](#).
- [43] H. Song and X. Wan, “Matching the real Higgs triplet extension of Standard Model to HEFT.” [arXiv:2503.00707](#).
- [44] T. Cohen, N. Craig, X. Lu, and D. Sutherland, “Is SMEFT Enough?” *JHEP* **03** (2021) 237 [[arXiv:2008.08597](#)].
- [45] R. Gómez-Ambrosio, F. J. Llanes-Estrada, A. Salas-Bernárdez, and J. J. Sanz-Cillero, “Distinguishing electroweak EFTs with  $WLWL \rightarrow n \times h$ ,” *Phys. Rev. D* **106** (2022) 053004 [[arXiv:2204.01763](#)].
- [46] R. Gómez-Ambrosio, F. J. Llanes-Estrada, A. Salas-Bernárdez, and J. J. Sanz-Cillero, “SMEFT is falsifiable through multi-Higgs measurements (even in the absence of new light particles),” *Commun. Theor. Phys.* **75** (2023) 095202 [[arXiv:2207.09848](#)].
- [47] A. Salas-Bernárdez, J. J. Sanz-Cillero, F. J. Llanes-Estrada, and R. Gomez-Ambrosio, “SMEFT as a slice of HEFT’s parameter space,” *EPJ Web Conf.* **274** (2022) 08013 [[arXiv:2211.09605](#)].
- [48] R. L. Delgado, R. Gómez-Ambrosio, J. Martínez-Martín, A. Salas-Bernárdez, and J. J. Sanz-Cillero, “Production of two, three, and four Higgs bosons: where SMEFT and HEFT depart,” *JHEP* **03** (2024) 037 [[arXiv:2311.04280](#)].
- [49] S. Mahmud and K. Tobioka, “Energy Growth in  $V_L V_L \rightarrow V_L V_L$ ,  $V_L V_L h$  Scattering to Probe Higgs Cubic and HEFT Interactions.” [arXiv:2406.03522](#).
- [50] X. Li, D. Zhang, and S. Zhou, “One-loop matching of the type-II seesaw model onto the Standard Model effective field theory,” *JHEP* **04** (2022) 038 [[arXiv:2201.05082](#)].

- [51] M. A. Schmidt, “Renormalization group evolution in the type I+ II seesaw model,” *Phys. Rev. D* **76** (2007) 073010 [[arXiv:0705.3841](#)]. [Erratum: *Phys.Rev.D* 85, 099903 (2012)].
- [52] P. S. Bhupal Dev, D. K. Ghosh, N. Okada, and I. Saha, “125 GeV Higgs Boson and the Type-II Seesaw Model,” *JHEP* **03** (2013) 150 [[arXiv:1301.3453](#)]. [Erratum: *JHEP* 05, 049 (2013)].
- [53] **Particle Data Group** Collaboration, “Review of Particle Physics,” *PTEP* **2022** (2022) 083C01.
- [54] J. Fuentes-Martín, M. König, J. Pagès, A. E. Thomsen, and F. Wilsch, “A proof of concept for matchete: an automated tool for matching effective theories,” *Eur. Phys. J. C* **83** (2023) 662 [[arXiv:2212.04510](#)].
- [55] V. Shtabovenko, R. Mertig, and F. Orellana, “New Developments in FeynCalc 9.0,” *Comput. Phys. Commun.* **207** (2016) 432–444 [[arXiv:1601.01167](#)].
- [56] R. Mertig, M. Bohm, and A. Denner, “FEYN CALC: Computer algebraic calculation of Feynman amplitudes,” *Comput. Phys. Commun.* **64** (1991) 345–359.
- [57] **ATLAS** Collaboration, “Constraints on the Higgs boson self-coupling from single- and double-Higgs production with the ATLAS detector using pp collisions at s=13 TeV,” *Phys. Lett. B* **843** (2023) 137745 [[arXiv:2211.01216](#)].
- [58] **CMS** Collaboration, “A portrait of the Higgs boson by the CMS experiment ten years after the discovery.” *Nature* **607** (2022) 60–68 [[arXiv:2207.00043](#)]. [Erratum: *Nature* 623, (2023)].
- [59] C.-W. Chiang, T. Nomura, and K. Tsumura, “Search for doubly charged Higgs bosons using the same-sign diboson mode at the LHC,” *Phys. Rev. D* **85** (2012) 095023 [[arXiv:1202.2014](#)].
- [60] S. Ashanujjaman and K. Ghosh, “Revisiting type-II see-saw: present limits and future prospects at LHC,” *JHEP* **03** (2022) 195 [[arXiv:2108.10952](#)].